Chapter 5
Results and Discussion

In this chapter we show our fitting results for three very different data sets. In addition to studying energetic heavy ions from the Sun, we also consider data on energetic protons, which have very similar dynamical properties; these additional data sets have posed interesting challenges and helped us to further improve our fitting techniques. In this work, we study particle data of interest from three solar events as discussed in the following sections.

We fit data for the various solar events in order to study

1. the mean free path, λ, of the particles released from the Sun as a function of energy and species, which is important for learning more about the interplanetary medium (Bieber et al. 1994), and

2. the injection profile as a function of time, energy and species, indicating the duration of injection (acceleration) and giving information on the mechanism of acceleration.

In addition, we aim to test our new and improved fitting techniques, which are the first to use automated fitting techniques to accurately determine the injection of particles near the Sun as a function of time and energy. The fits are objective, relying on χ^2 minimization, whereas previous fits have been evaluated by eye. Section 5.4 compares and contrasts the results from these three solar events.

5.1 The Solar Event on July 9, 1996

For the solar event on July 9, 1996, we have fit data from the WIND spacecraft. The data were prepared by Wolfgang Dröge and his collaborators. He invited us to fit these data for comparing with his fitting results (he uses very different techniques). These data represent the anisotropy and intensity of protons at 123 keV.

The corresponding solar wind velocity is 420 km/s as shown in Figure 5.1, which gives details about the parameters of the solar wind, such as the magnitude of the solar wind velocity, its density, thermal speed, direction angle to the West (−) or East (+), and to the South (−) or North (+) (bottom panel to top panel, respectively). The solar wind speed is an input value for the simulation program. The X-ray intensity level is X2 as shown in Figure 5.2, where the standard notation uses X, M, C, B, and A to represent the order of magnitude of the X-ray intensity from 10^{-4} to 10^{-8} W/m^2, respectively. The X-ray profile data are useful for classification of solar events. If the X-ray duration is short, it is an impulsive solar event, or if the X-ray duration is long, $>$ 10 min, it is a gradual solar event, where the X-ray duration is given by the e-folding decay time of the X-ray emission (Cliver et al. 1989). If instead the X-ray duration is defined at 10% of its peak intensity, it is $<$ 1 hour for an impulsive event (Pallavicini et al. 1977, Cane et al. 1986). The X-ray duration time for this event (decay time) is about 5 min (Laitinen et al. 2000), which implies that this is an impulsive event.

This fitting was performed by the author in collaboration with Mr. Varutm Hongskul (2000). These data are at a very low particle energy, at which the particle velocity is only seven times higher than the solar wind speed. The old version

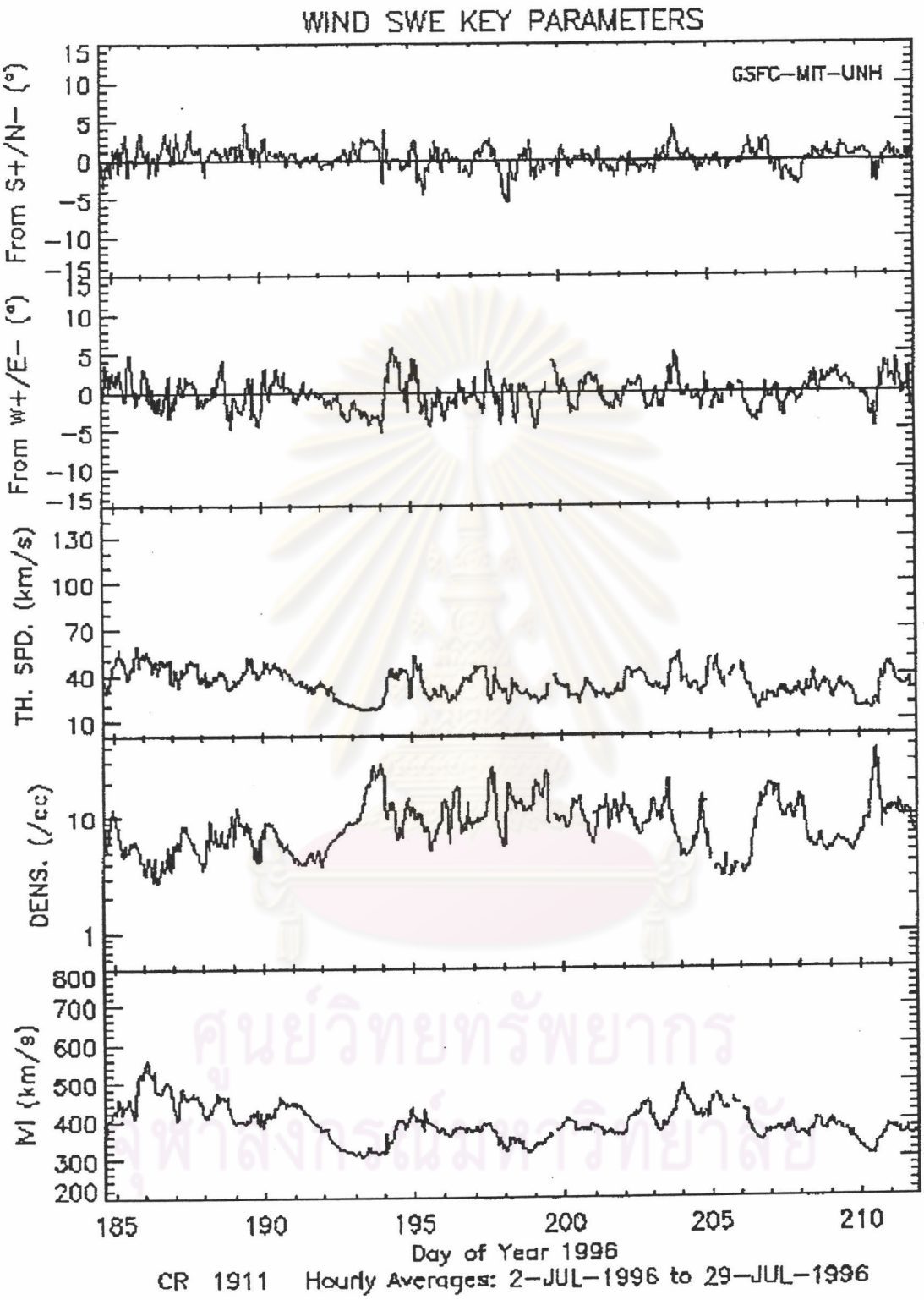

Figure 5.1: Solar wind parameters from the WIND spacecraft on July 2-29, 1996. The event of interest is on July 9, or day of year (doy) = 191. Downloaded from http://web.mit.edu/space/www/wind.

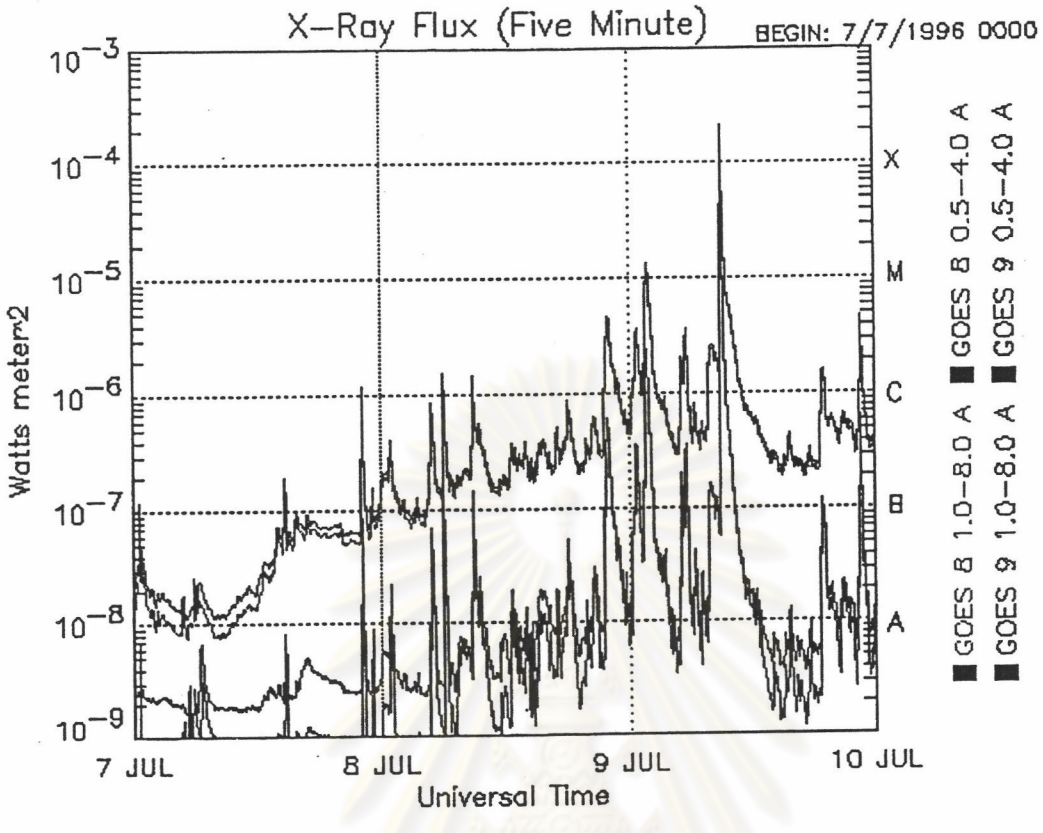

Figure 5.2: The X-ray flux profile on July 7-9, 1996, downloaded from http://solar.sec.noaa.gov/ftpmenu/plots.html

of our programs considered the case of particles which have a velocity much higher than the solar wind speed, so we needed to develop our program for finding the intensity and anisotropy of particles by properly evaluating the Compton-Getting effect, transforming the intensity and anisotropy of particles from the solar wind frame to the observer's frame.

In preparing the data for fitting (Figure 5.3 and 5.4), we employed our new technique for evaluating uncertainties, taking interplanetary fluctuations into account. We found that the interplanetary fluctuations in the intensity data are much higher than in the |anisotropy|×intensity, which is an interesting observation regarding low energy solar particles. The fitting results are as follows: We

obtain a best-fit mean free path value, $\lambda_r = 0.4279$ AU, with statistical error 0.0073 AU, giving fitting results close to the spacecraft data at $\chi^2 = 224.6$ for 154 degrees of freedom, as shown in Figures 5.3 and 5.4. Wolfgang Dröge got $\lambda_{||} = \lambda_r \sec^2 \psi$ of about 0.8 AU, which close to our results (we got $\lambda_{||} = 0.8558$ AU), so we consider this comparison of fitting results to be successful. The full width at half maximum (FWHM) injection time of the event is 274 min as indicated in Figure 5.5. Such a long duration of injection is consistent with the identification as a gradual solar event.

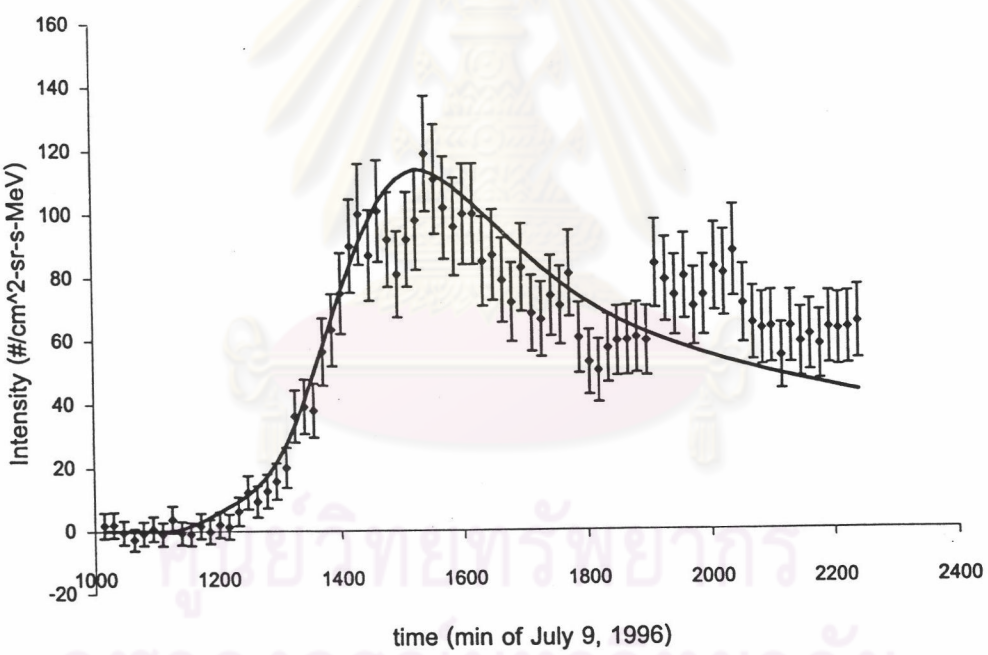

Figure 5.3: The intensity fitting results for protons at 123 keV from the WIND spacecraft on July 9, 1996. Diamonds indicate the data with uncertainties, and the line indicates the fit.

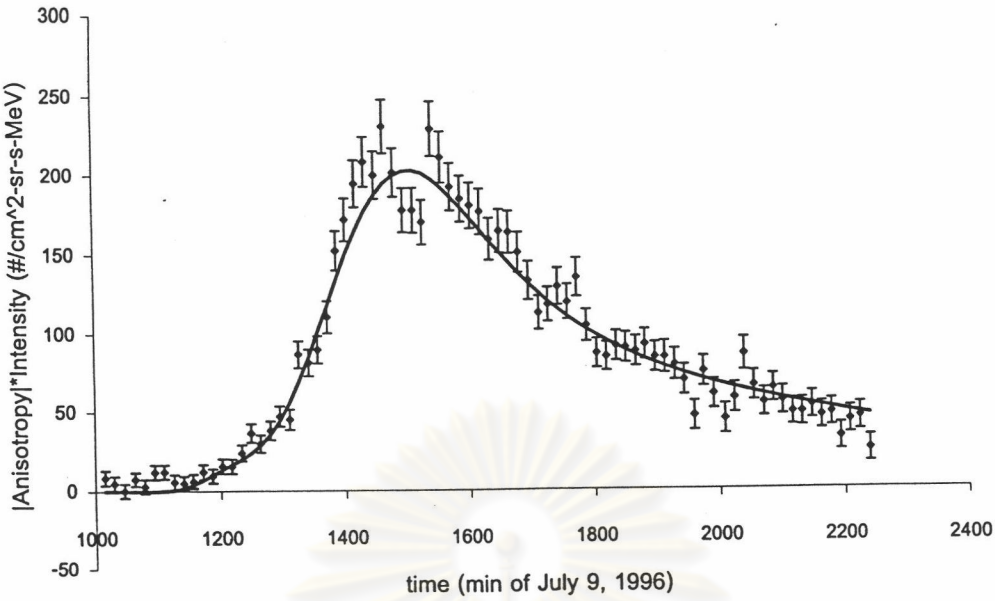

Figure 5.4: The anisotropy fitting results for protons at 123 keV from the WIND spacecraft on July 9, 1996. Diamonds indicate the data with uncertainties, and the line indicates the fit.

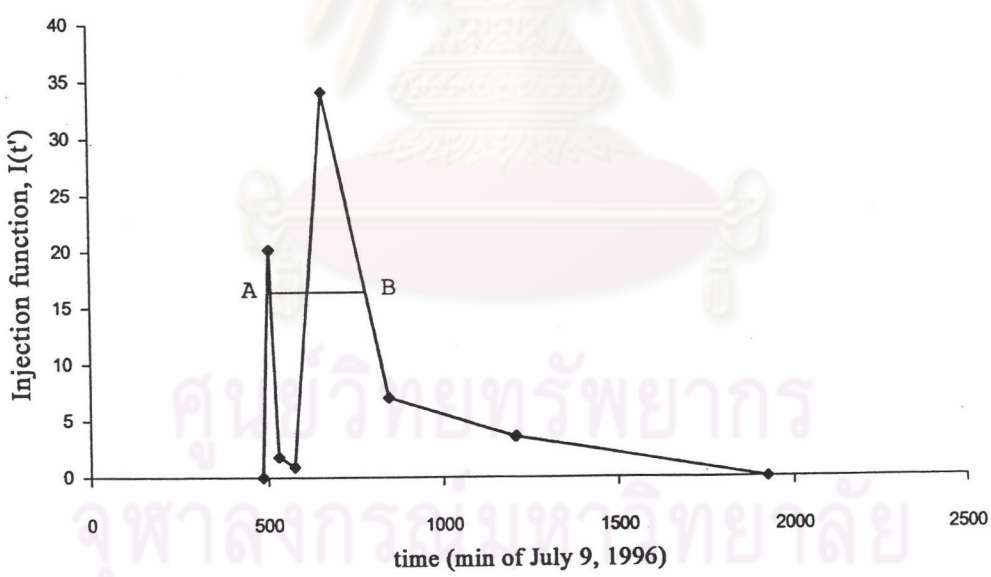

Figure 5.5: The injection function of protons at 123 keV of the solar event on July 9, 1996 at λ_r= 0.42 AU, in which the injection time is 274 min from point A to B.

5.2 The Solar Event on July 14, 2000

We have also fitted data from the solar event on July 14, 2000 (sometimes called the Bastille Day event after the French holiday on July 14). This event was the strongest of the present solar cycle (since 1991), and there was a coronal mass ejection (CME). There have been several other journal or conference papers published about this event (Tylka et al. 2001, Reames et al. 2001, Klein et al. 2001, Yan et al. 2001) which have examined the acceleration in a large gradual event by the CME-driven shock, and reported about the radio source indicating electron acceleration and the magnetic field reconfiguration in the western hemisphere, in which the radio source is close to the Earth-connected interplanetary magnetic field line.

The data set is from ground-based neutron monitors around the world. The primary solar energetic particles are mostly protons with a mean rigidity ~2.15 GV. John W. Bieber, Wolfgang Dröge, Paul A. Evenson, and Roger Pyle at the Bartol Research Institute, University of Delaware, Newark, DE, USA prepared the proton intensity and anisotropy data for this event, and invited us to join in fitting the data. As a "double blind" test, we (research term at Chulalongkorn University) and Wolfgang Dröge individually fit for comparing fitting results. Thus the goals of our fitting were to determine the mean free path of the particles and their injection function, and to confirm the accuracy of our fitting technique.

The location of the flare on the Sun's surface was determined by ground-based observations of the Hα line of hydrogen. The location is expressed as degrees latitude (relative to the Solar Equator) and degrees longitude (relative to the Central Meridian). The Bastille Day event occurred at N22W07. The X-ray class is X5 as shown in Figure 5.6. The corresponding solar wind velocity near

Earth was not actually measured because of a data gap (see Figure 5.7), so we estimate it to be 500-700 km/s, and use 600 km/s be the input value for the solar wind speed in our simulation.

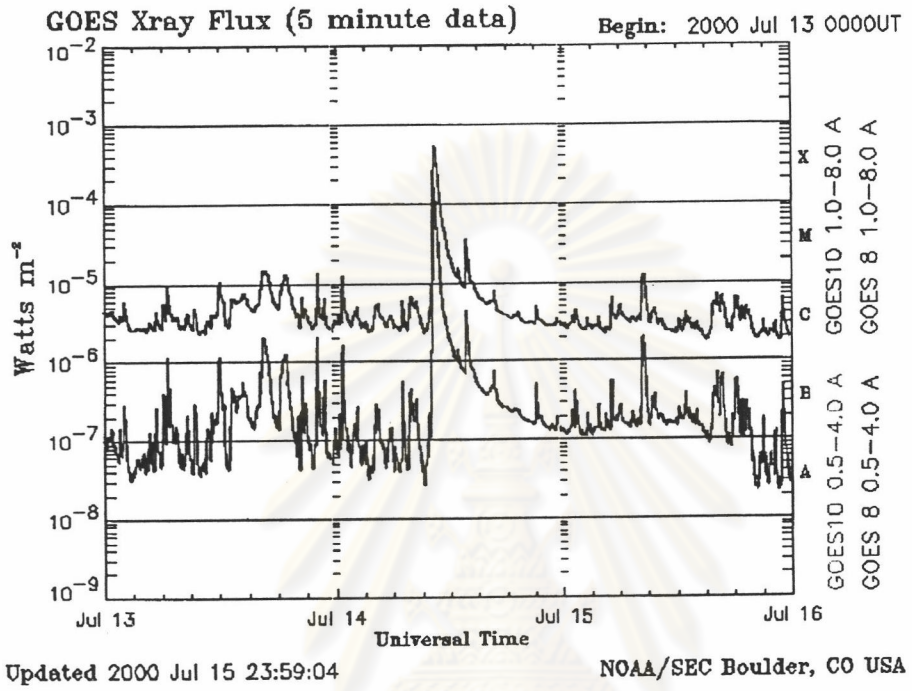

Figure 5.6: The X-ray flux profile on July 13-15, 2000.

First we simulated the particle transport by numerically solving the equation of Ruffolo (1995), and then we fit the simulation results to the selected data. We found that fitting results were good for intensity data, but did not give a good fit for |anisotropy|×intensity data, as shown in Figures 5.8 and 5.9. (Actually, we fit the quantity |anisotropy|×intensity because our fitting technique uses linear least squares fitting and requires the superposition principle for |anisotropy|×intensity ≈ anisotropy×intensity.) The fast decay of the |anisotropy|×intensity cannot be fit by our usual transport model. Thus we must consider other influences that might have occurred in the interplanetary medium

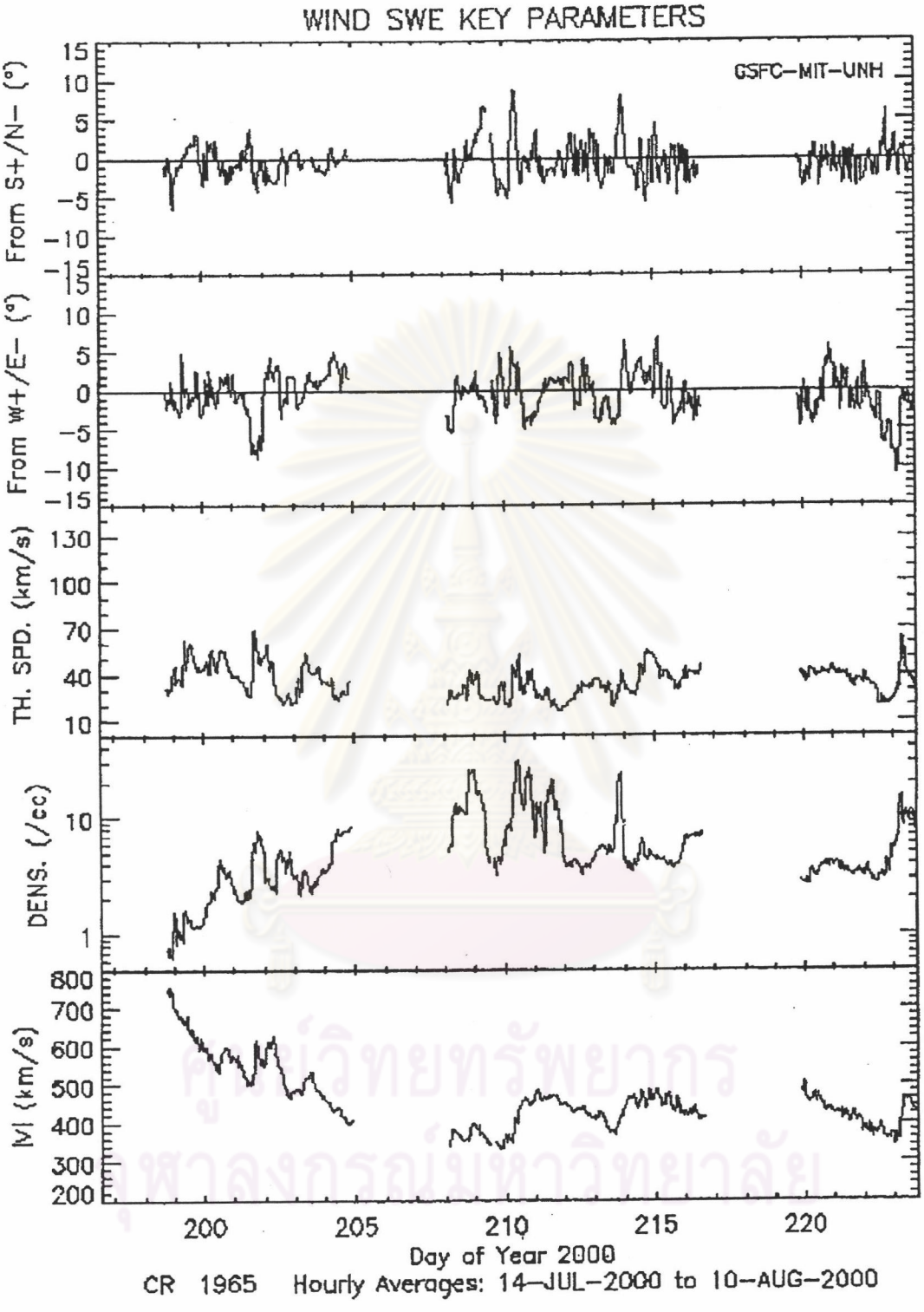

Figure 5.7: Solar wind parameters measured near Earth by the WIND spacecraft on July 14 to August 10, 2000. The event of interest is on July 14, or day of year (doy) = 196.

during the time of this event.

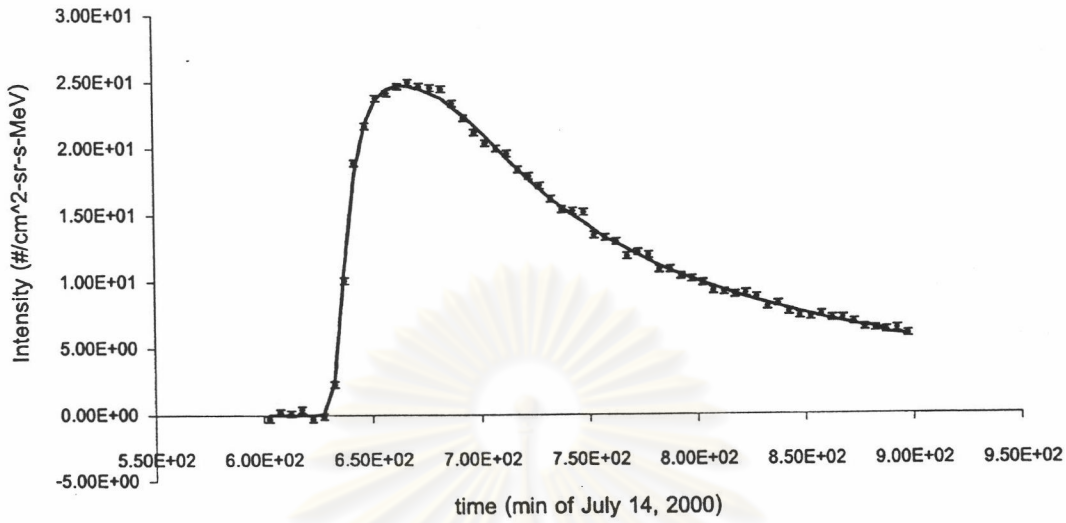

Figure 5.8: The intensity fitting results for protons on July 14, 2000 before adding the bottleneck configuration. Points indicate data, with uncertainties, and the line represents the fit.

After looking at the magnetic field data, we found that there were magnetic field jumps because of various CMEs, including a jump at about 15:00 UT on July 14, 2000 due to a CME released from the corona on July 11, 2000. This influence from the CME should also have affected the shape of the magnetic field lines as shown in Figure 5.10. We refer to this configuration as a "bottleneck." Because of magnetic mirroring, some particles will pass through the bottleneck but most will be reflected back toward the Sun. We added the process of magnetic mirroring, which is the effect of the bottleneck configuration of the magnetic field lines, into the transport equation. The process of magnetic mirroring (also called adiabatic focusing) conserves the magnetic moment, $p^2(1-\mu^2)/(2meB)$. We find the minimum value of μ for which particles can pass through the bottleneck to be $R = \sqrt{1-1/r}$, where r is the maximum magnetic compression, and R represents the fraction of particles reflected by magnetic mirroring, or a reflection coefficient.

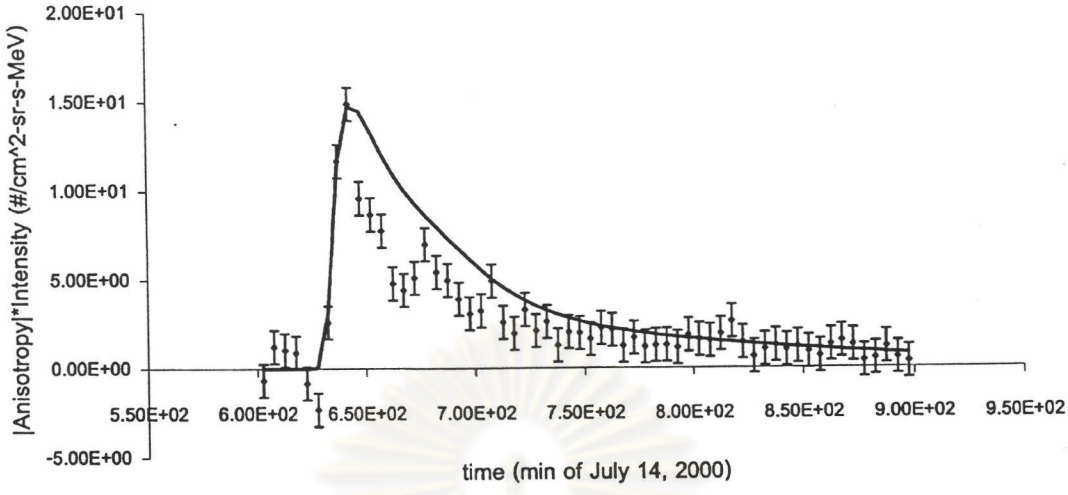

Figure 5.9: The anisotropy fitting results for protons on July 14, 2000 before adding the bottleneck configuration.

We take the effect of magnetic mirroring into account by modifying the transport equation of Ruffolo (1995). We add a compression in $\ln B$ of Gaussian form to that for an Archimedean spiral magnetic field:

$$\ln B = (\ln B)_{\text{Arch}} + \eta \exp\left[-\frac{(r-r_0)^2}{2\sigma^2}\right] \tag{5.1}$$

$$\frac{1}{L} = -\frac{d}{dz}\ln B \tag{5.2}$$

$$= \left(\frac{1}{L}\right)_{\text{Arch}} + \eta\cos\psi\frac{r-r_0}{\sigma^2}\exp\left[-\frac{(r-r_0)^2}{2\sigma^2}\right], \tag{5.3}$$

where "Arch" indicates an uncompressed Archimedean spiral field, r_0 is the heliocentric distance at the center of bottleneck, ψ is the angle between $\hat{r}$ and $\hat{z}$, σ is the width of the bottleneck, η is the amplitude, and R is the reflection coefficient. Our simulation results now give the rapid declining anisotropy. This work is the first to present about the focused transport for a magnetic bottleneck inside the simulation region.

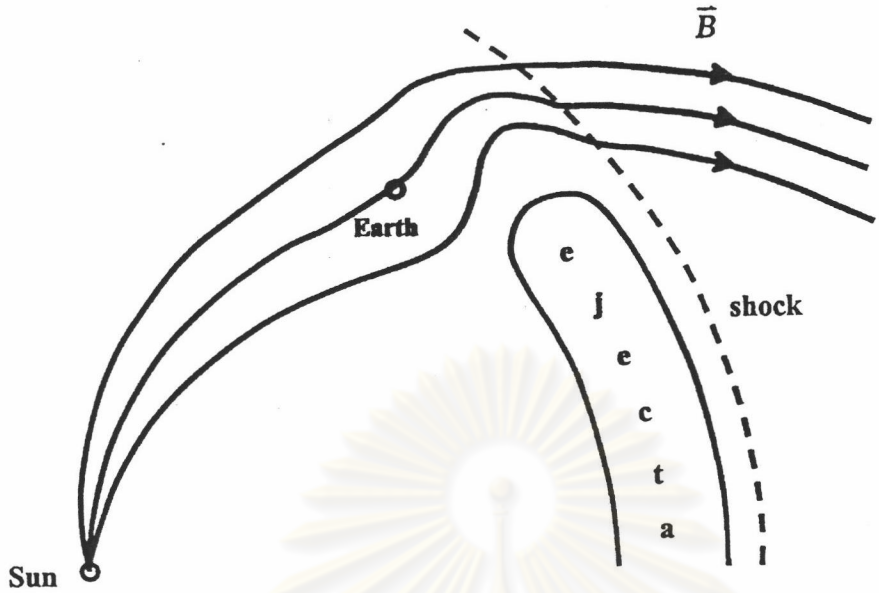

Figure 5.10: The configuration of magnetic field lines from the Sun to the Earth, with the bottleneck.

The fitting results after using the bottleneck configuration are better than the old version. The new simulation results for the anisotropy are closer to the anisotropy data, in particular to the rapidly declining anisotropy. The best-fit results give the minimum χ^2 when we define $R = 0.8$, and r_0 was set to 1.3 AU, which is close to the value expected from the magnetic field data. These results can explain the effects of the bottleneck in the magnetic field structure as well. The best mean free path for this event from the fitting results is 0.18 AU, after we set the reflection coefficient to 85%. The injection time has a FWHM of 7 min. These results are shown in Figures 5.11-5.13.

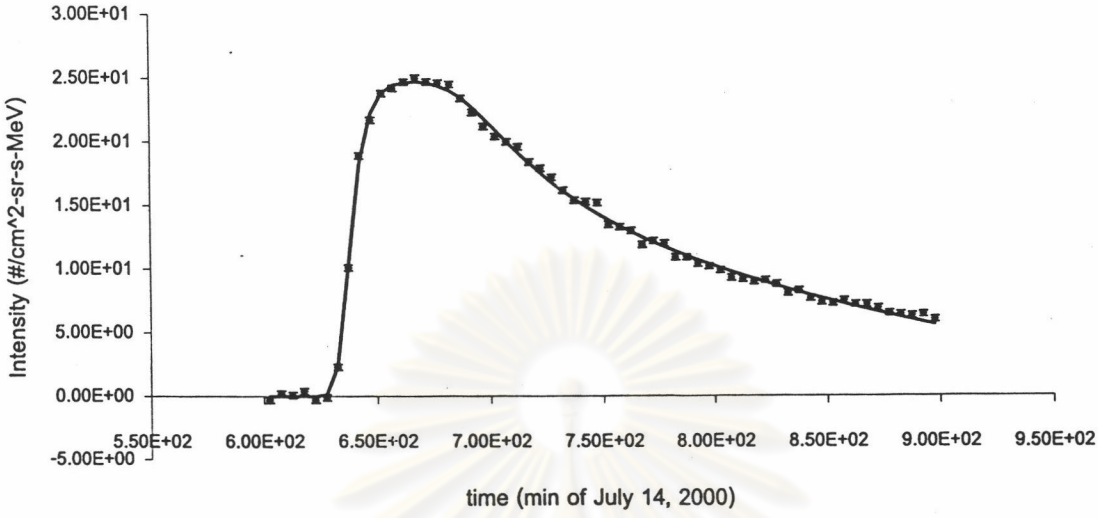

Figure 5.11: The intensity fitting results for protons on July 14, 2000 after adding the bottleneck configuration for λ= 0.18 AU.

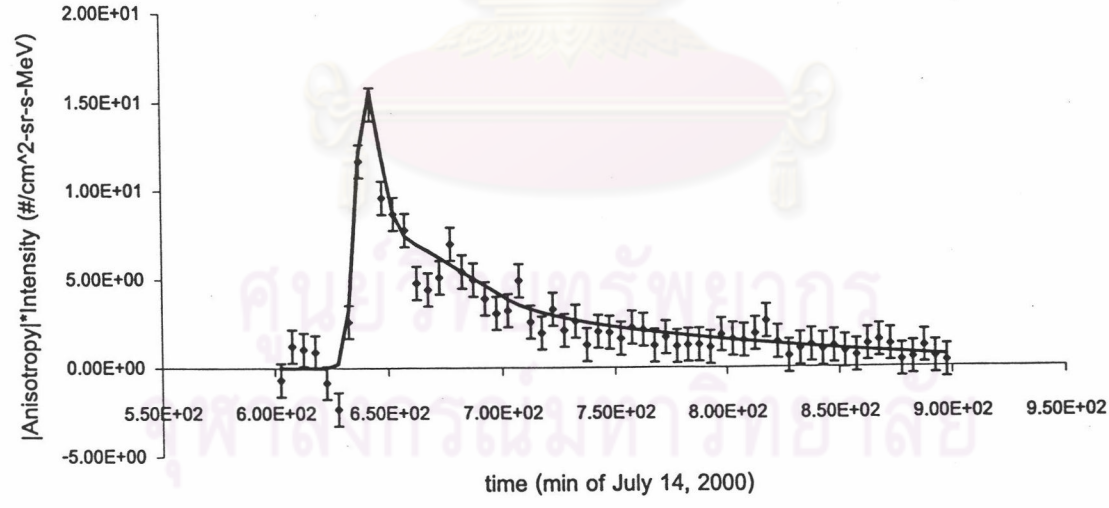

Figure 5.12: The anisotropy fitting results for protons on July 14, 2000 after adding the bottleneck configuration for λ= 0.18 AU.

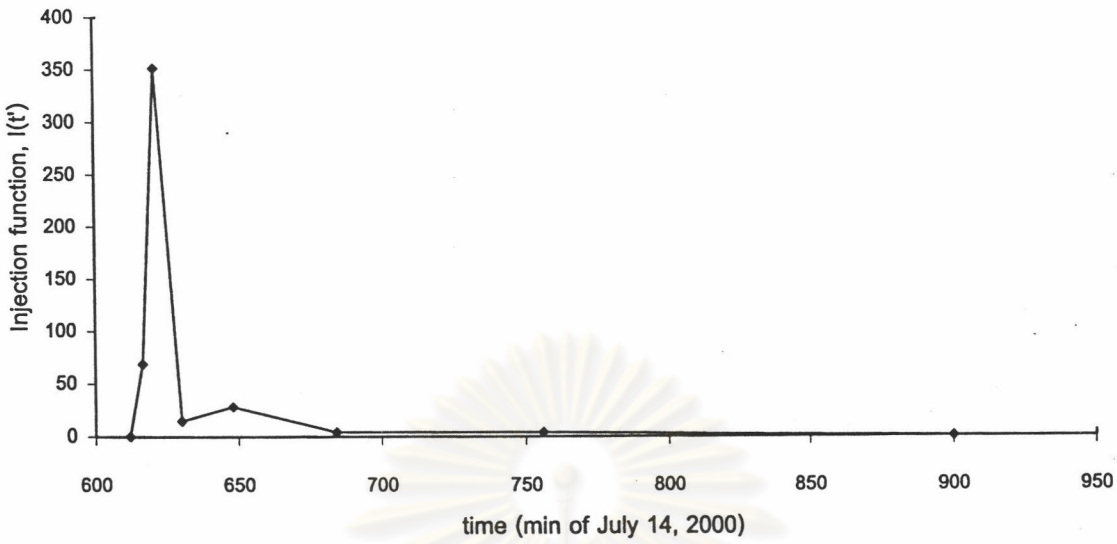

Figure 5.13: The injection profile with FWHM of 7 min for the solar event on July 14, 2000.

We confirmed our fitting results with those of Wolfgang Dröge and we got approximately the same mean free path and injection time for protons measured by neutron monitors on July 14, 2000. For this event, we have also learned something new about the interplanetary transport of cosmic rays. In this work we have subjected our fitting technique to a test against the other fits as a "double-blind" experiment, in which researchers used the separate techniques for fitting and simulation for this event. This work provides important evidence for the explanation of mirroring in the magnetic field structure and the reflection of solar particles from a magnetic bottleneck beyond the Earth. This work has been published in the Astrophysical Journal of March 1, 2002 (vol. 567, pp. 622-634).

5.3 Solar Event on November 6, 1997

In Figure 5.14 shows oxygen intensities from the ULEIS and SIS instruments on board the ACE spacecraft during November 4-6, 1997, a time interval which had 2 major solar events. The first flare occurred at 05:54 UT on Nov. 4, 1997 (doy=308), and the associated CME-driven shock was observed to pass near the Earth at 22:00 on Nov. 6, 1997 (doy=310). The second flare occurred at 11:22 on Nov. 6 (doy=310), and its shock was observed at ~10:00 on Nov. 9 (doy=313). The eruption of the second flare produced a "ground level enhancement" (GLE) in ground-based detectors (neutron monitors). We see that the first shock, with the associated peak in low energy intensity, nearly coincided with the increasing phase of the Nov. 6, 1997 event. After the solar flare eruption, the solar energetic particles disperse into interplanetary medium, where the higher energy particles arrive at the Earth faster than the lower energy particles, as shown in Figure 5.14 for the time-intensity profile of particles at 3.84-49.6 MeV/n, where their time-intensity profiles correspond to the injection of particles at or near the Sun. We also observe the effects of the first CME on the time-intensity profiles of particles at 0.06-1.92 MeV/n. We found that the time-intensity profiles of particles up to ~2 MeV/n suddenly increased at the same time with distortions of the intensity, whereas the arrival time at Earth of the particles from an eruption at the Sun should be later as the energy decreases, so one can conclude that the enhancement of time-intensity profiles of particles up to ~2 MeV/n comes from the effects of the first CME-driven shock, not the second flare/CME. The effect of the second shock is associated with an increase in particle intensity on day 313 (Mason et al. 1999a).

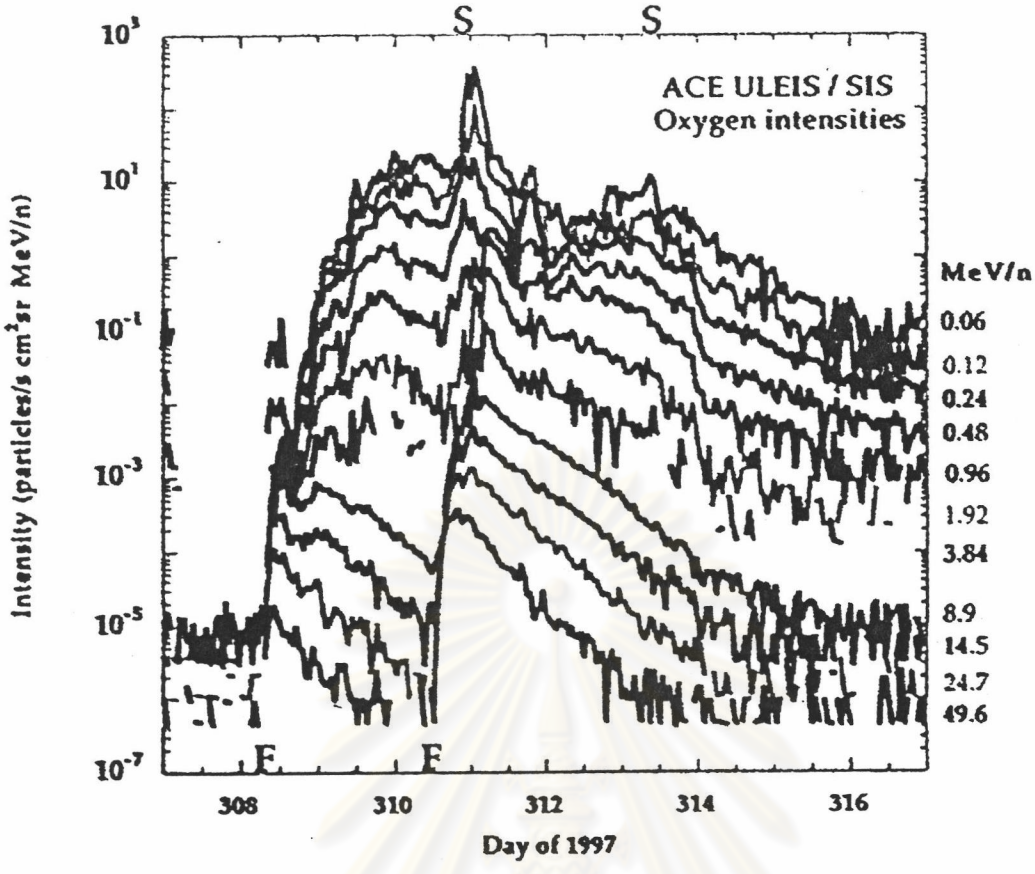

Figure 5.14: The hourly averaged oxygen intensity from 60 keV/n to 50 MeV/n from the ACE spacecraft due to the Nov. 4 and 6, 1997 events, where F is a flare time, S is a shock arrival time. (Mason et al. 1999a)

A typical impulsive solar event will release (or "inject") solar energetic particles over a short time duration, and soon thereafter they start arriving at the Earth (about 8 min later if traveling near the speed of light). The intensity vs. time profile quickly increases and decreases as a particles pass the Earth (Ruffolo & Khumlumlert 1995). On the other hand, a typical gradual event has a CME occurring at the same active region, which can drive a shock in the interplanetary medium. This greatly increases the number of energetic particles arriving at Earth, and can even cause a ground level enhancement, detectable by ground-based neutron monitors.

The Nov. 6 event was the first major solar event of the current solar

cycle, and attracted much attention, particularly in regard to SEP heavy ions of various energy ranges. For example, this is the only event for which the ionic charge state distribution and mean ionic charges have been observed to vary with energy in the sub-MeV range, and the ionic charge is an important parameter for understanding the acceleration and transport of the solar energetic particles (Möbius et al. 1999). This solar event has another point of interest. It showed an enhancement of Fe/O and the ratio of ^{3}He/^{4}He 4 times the coronal value (Mason et al. 1999a) which typically corresponds to an impulsive event, though there is an alternative explanation of such ratios in gradual events in terms of "contamination" of material from impulsive events (Mason et al. 1999b). This event had a CME at the same time which is a characteristic of gradual flares, as is the very high intensity of SEP and the CME-driven shock in interplanetary medium, which it indicates the gradual event. On the other hand, Cohen et al. (1999) inferred the mean charge states of elements. They found that mean charge states were high, which can be interpreted to indicate the high temperature of the source distribution near the flare site ($\sim 10^7$ K), and the Fe/O ratio was high (~ 1), which indicates an impulsive event, so some researchers claim that it is hard to classify this solar event as impulsive or gradual.

The solar flare event on November 6, 1997, was observed at the location on the Sun of S18W63 at 11:22 UT. This event has X9/2B class X-ray/Hα intensity as shown in Figure 5.15, with an X-ray duration at 10% of its peak intensity of < 1 hour (Cliver et al. 2001). While the decay to 10% of peak intensity was very fast, the X-ray flux took a very long time to decay completely after the start of the flare, which corresponds to a gradual flare (as explained in section 5.2). The solar wind velocity was 355 km/s as shown in Figure 5.16, from measurements

by the ACE spacecraft. The spacecraft data we studied were downloaded from http://www.srl.caltech.edu/ACE. This website has a large amount of data on solar events and the interplanetary medium as detected by the instruments on the ACE spacecraft. In this event we fit the intensity data for Si, Mg, Fe, O, and Ne from the SIS instrument on the ACE spacecraft, for which SIS detected the isotopic composition of energetic nuclei from He to Ni (Z = 2 to 28) over the energy range from ~10 to ~100 MeV/nucleon. Our analysis was authorized by M. Wiedenbeck on behalf of the SIS collaboration.

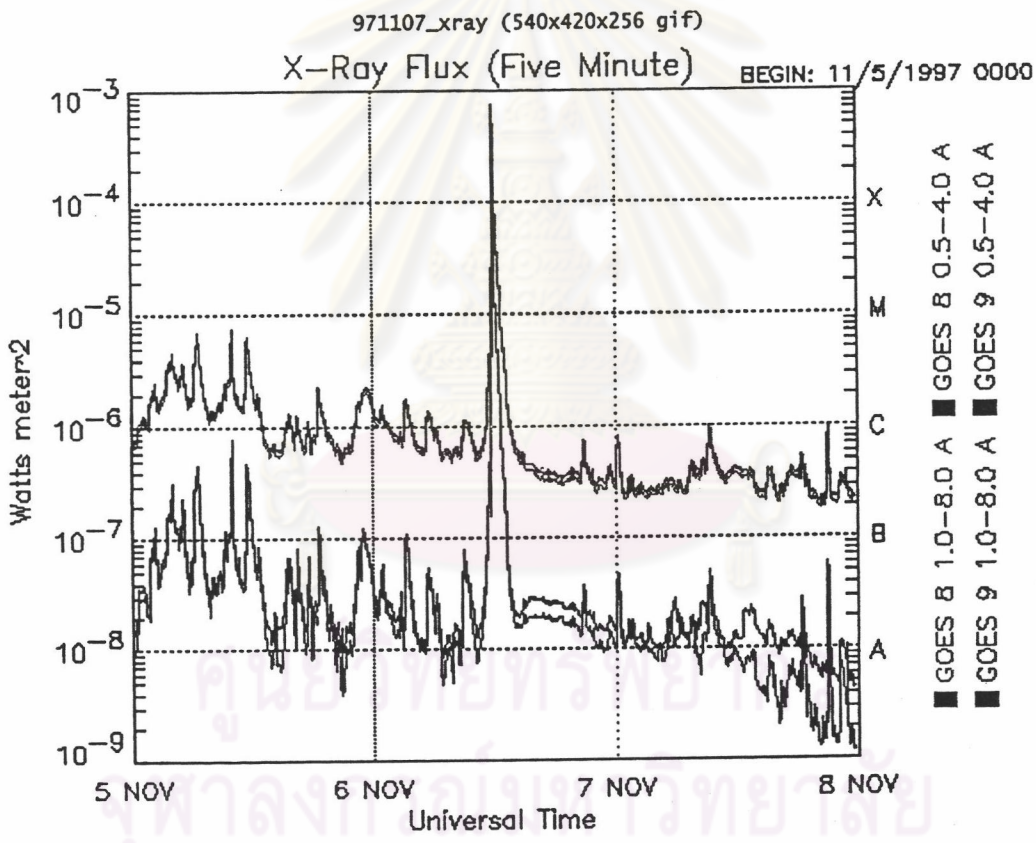

Figure 5.15: The X-ray flux profile on November 6, 1997.

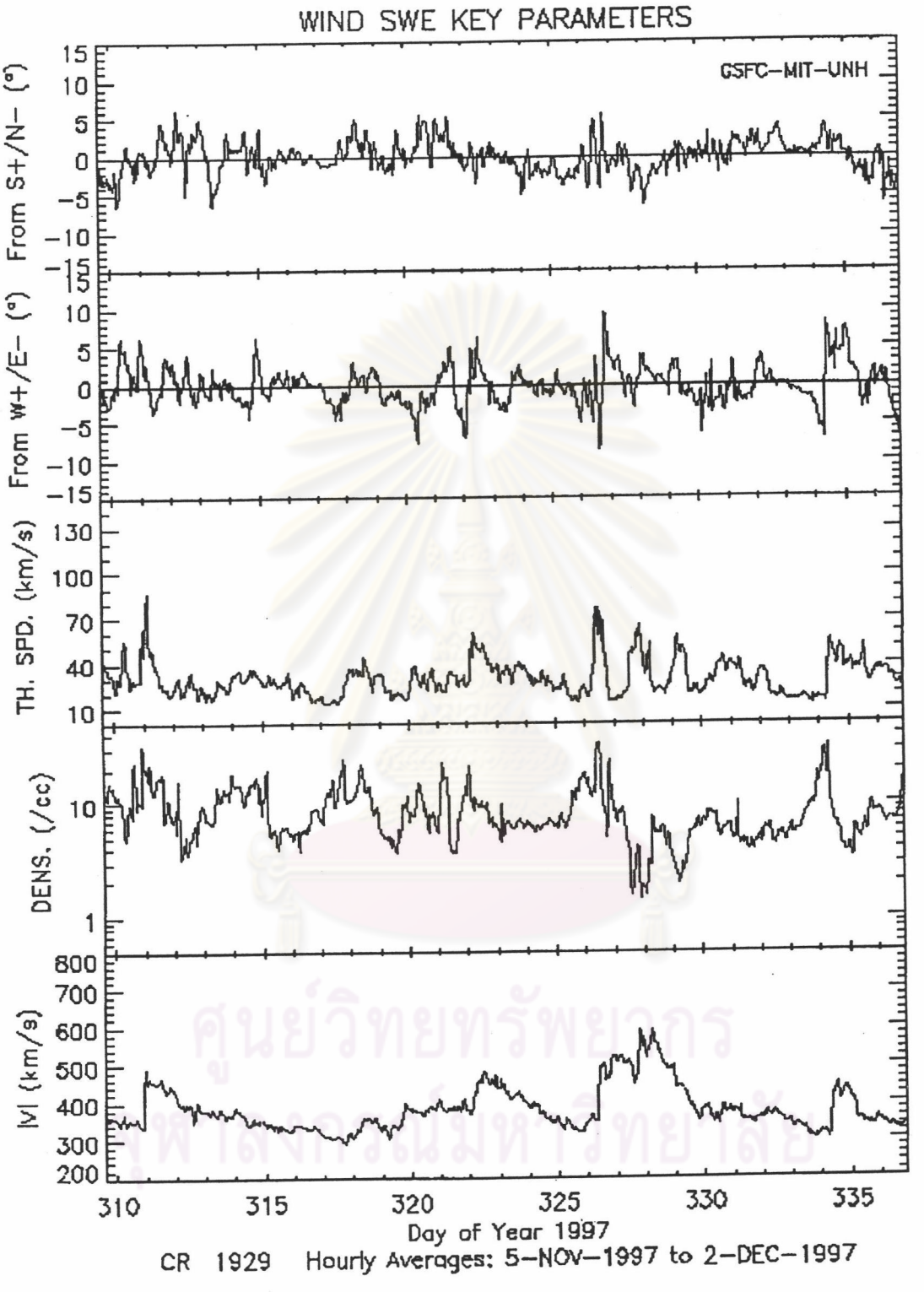

Figure 5.16: The solar wind parameters from the WIND spacecraft on November 5 to December 2, 1997. The event of interest is on November 6, or day of year (doy) = 310.

For this event, we fit the intensity data of interest with their uncertainties (which include the interplanetary fluctuations) with the results from the simulation program, which is based on the transport equation of Ruffolo (1995) with the technique of linear least squares fitting and an automatic truncation of the piecewise linear injection function. In this work we analyze the fitting results for various elements and energy bands. We believe that this is the most extensive fitting of such SEP data ever performed. For this event, we have only obtained intensity data for the particles of interest from SIS. In the future, if the experimental group is willing to prepare anisotropy data for us, our fitting results will be more reliable and complete.

We find the mean free path for a minimum χ^2 value between the fit and spacecraft data. Out of a total of 40 data sets, there are some (14) data sets which were difficult to fit, which meant that fluctuations of the data were very large, or there was more than one minimum χ^2 value as a function of the mean free path, and we could not find the most appropriate mean free path and injection function. Examples of fits for each element are shown in Figures 5.17-5.26, and details of all the remaining fits or fit attempts are shown in Appendices B and C.

In our results, the mean free path vs. energy for each element was nearly constant, as shown in Figure 5.27. The injection time for each element typically decreased with increasing energy as shown in Figure 5.28. The summary of the fitting results for this event is shown in Table 5.1, and we interpret the results further in the next section.

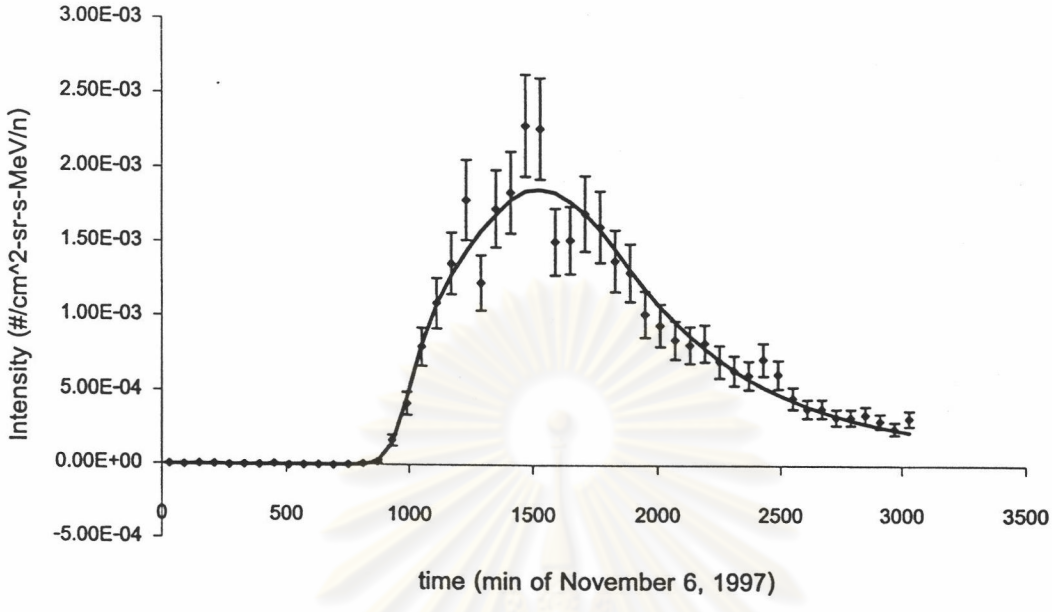

Figure 5.17: The intensity fitting result of oxygen at 15.6-21.0 MeV/n from the SIS instrument on the ACE spacecraft on November 6, 1997. The diamond symbols indicate data with their uncertainties, and the line represents the fit.

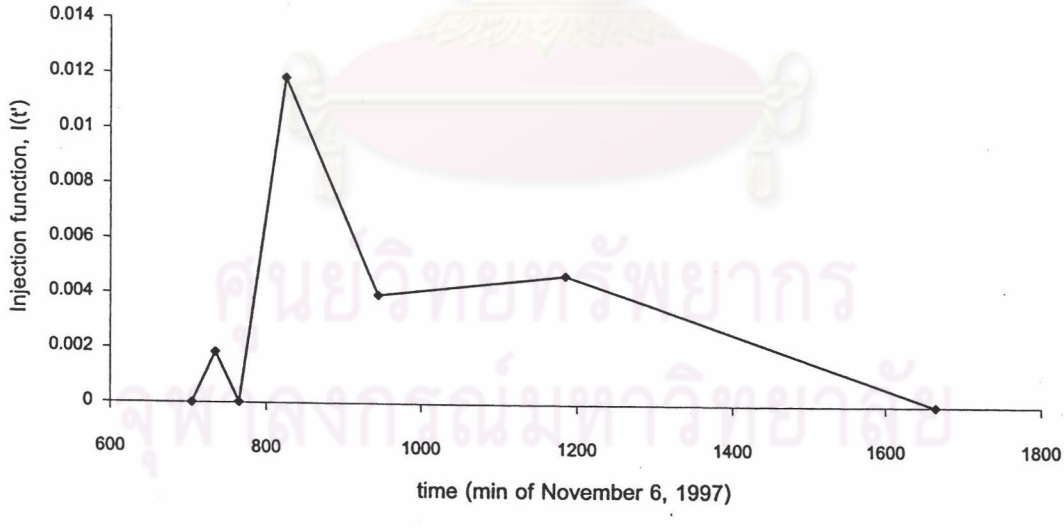

Figure 5.18: The injection function of oxygen at 15.6-21.0 MeV/n of the solar event on November 6, 1997 at the best-fit λ= 0.054 AU.

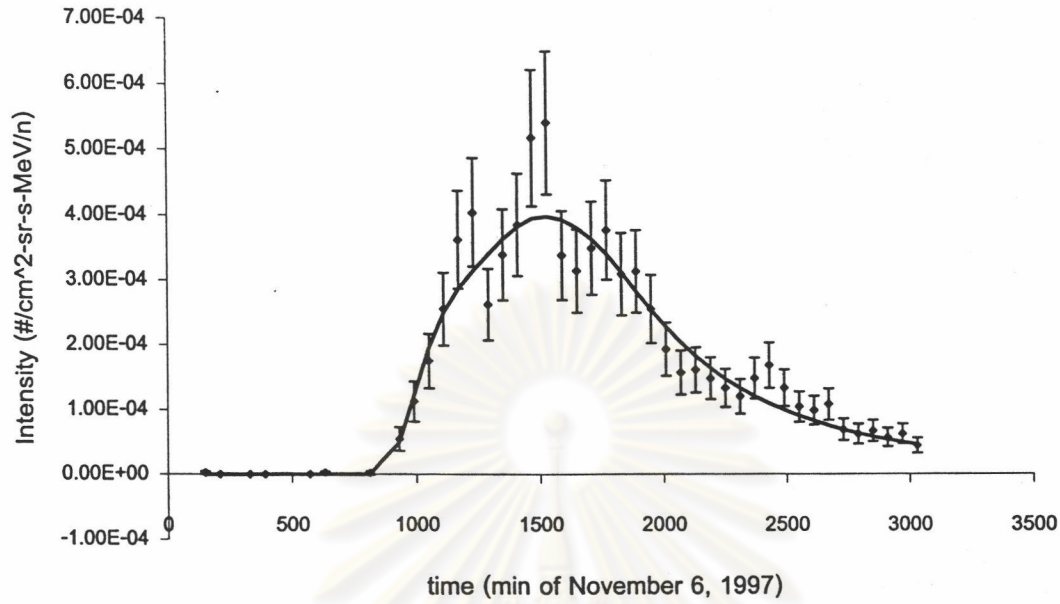

Figure 5.19: The intensity fitting result of neon at 17.6-23.6 MeV/n from the SIS instrument on the ACE spacecraft on November 6, 1997.

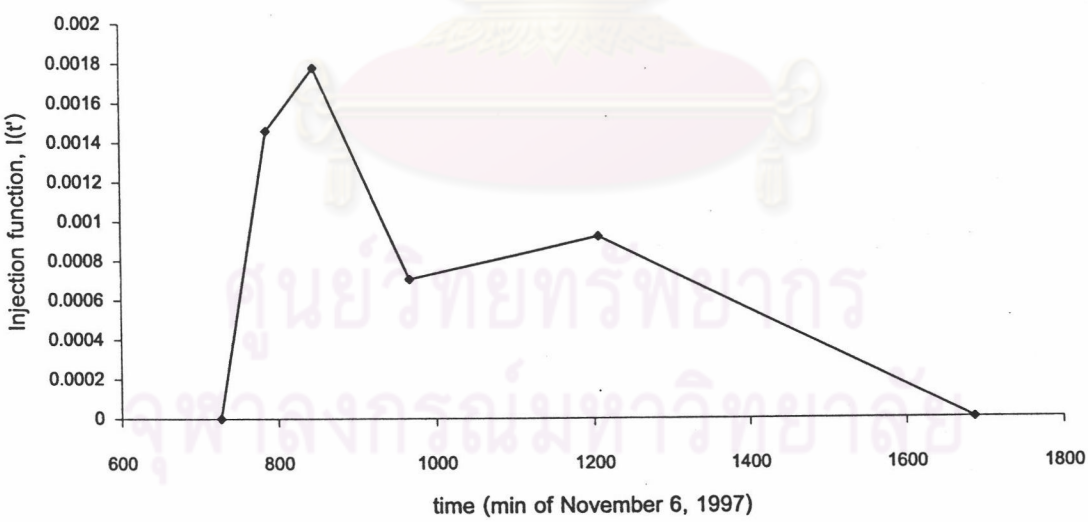

Figure 5.20: The injection function of neon at 17.6-23.6 MeV/n of the solar event on November 6, 1997 at the best-fit λ= 0.054 AU.

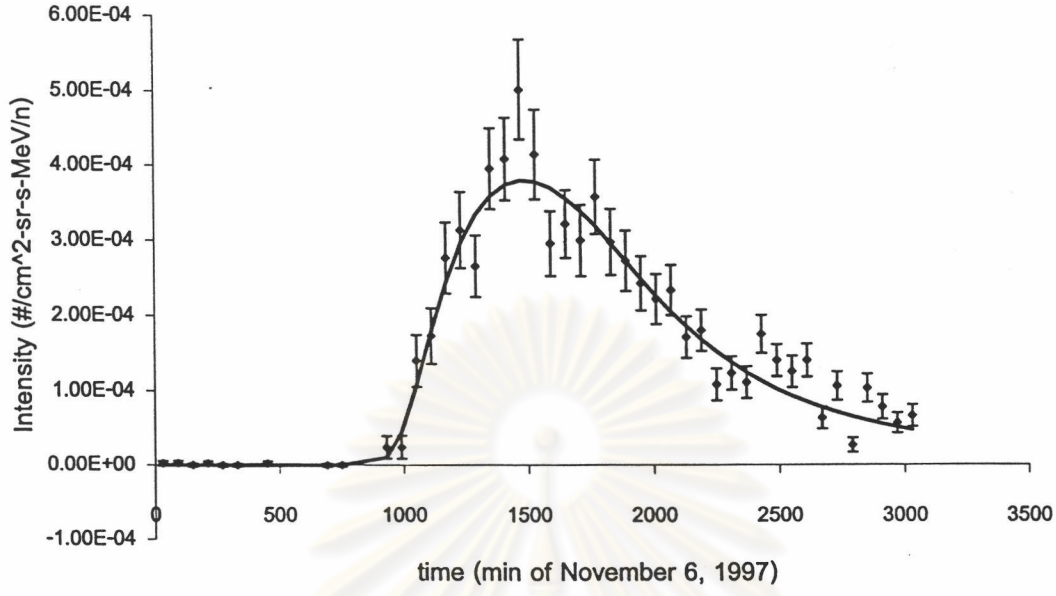

Figure 5.21: The intensity fitting result of magnesium at 16.0-19.3 MeV/n from the SIS instrument on the ACE spacecraft on November 6, 1997.

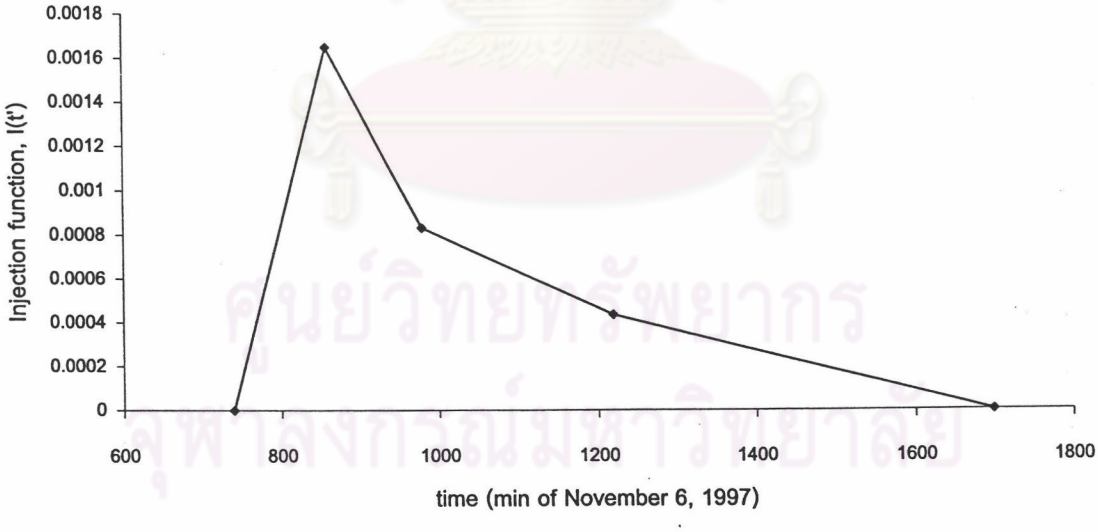

Figure 5.22: The injection function of magnesium at 16.0-19.3 MeV/n of the solar event on November 6, 1997 at the best-fit λ= 0.041 AU.

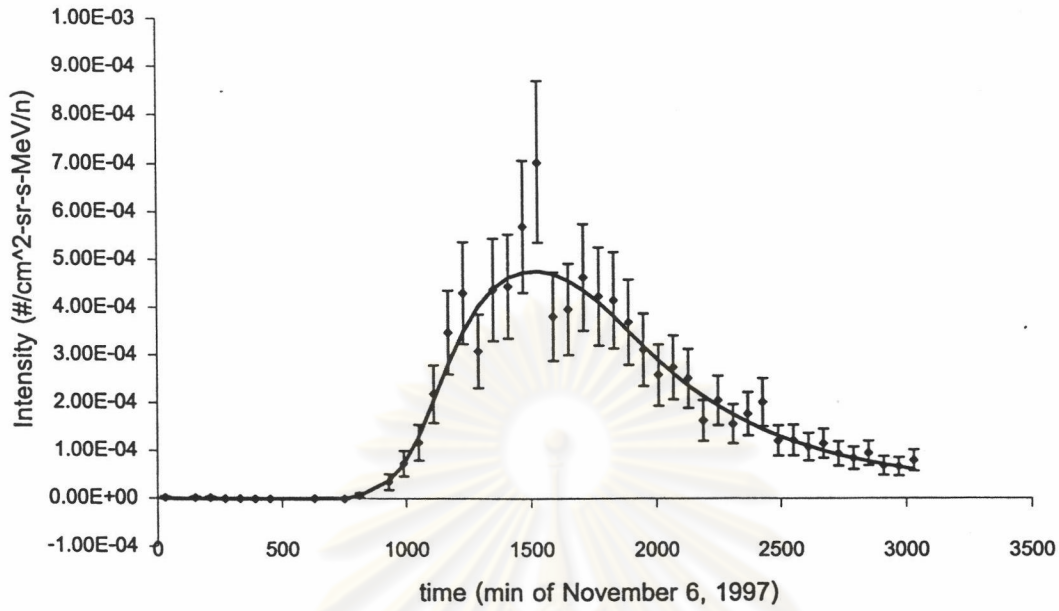

Figure 5.23: The intensity fitting result of silicon at 13.0-17.3 MeV/n from the SIS instrument on the ACE spacecraft on November 6, 1997.

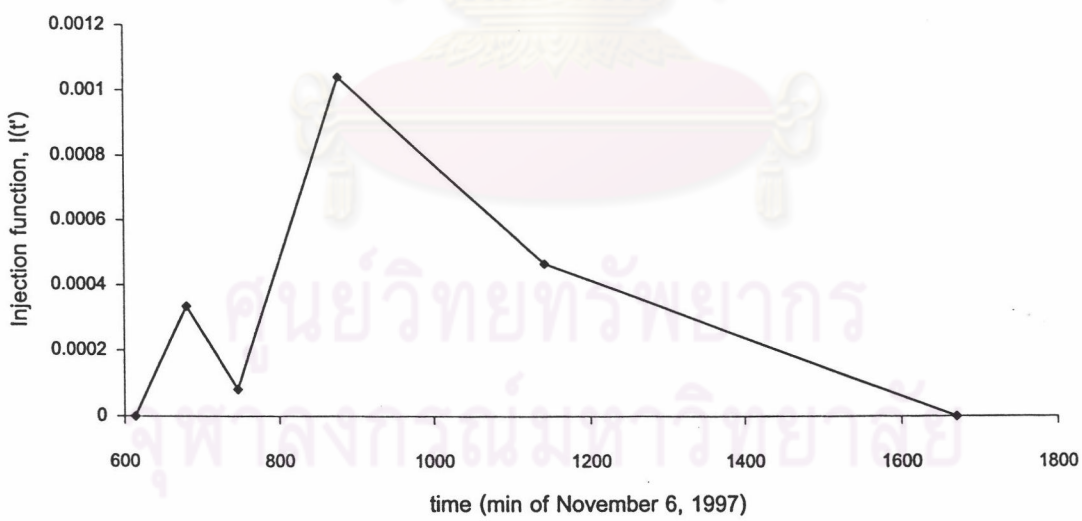

Figure 5.24: The injection function of silicon at 13.0-17.3 MeV/n of the solar event on November 6, 1997 at the best-fit λ= 0.042 AU.

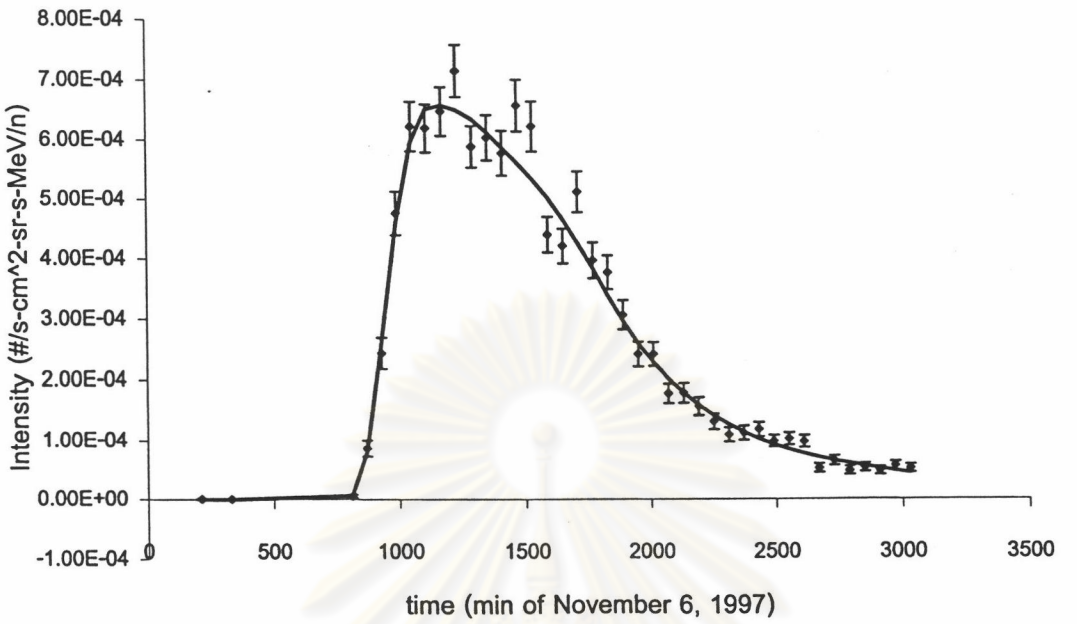

Figure 5.25: The intensity fitting result of iron at 23.6-36.3 MeV/n from the SIS instrument on the ACE spacecraft on November 6, 1997.

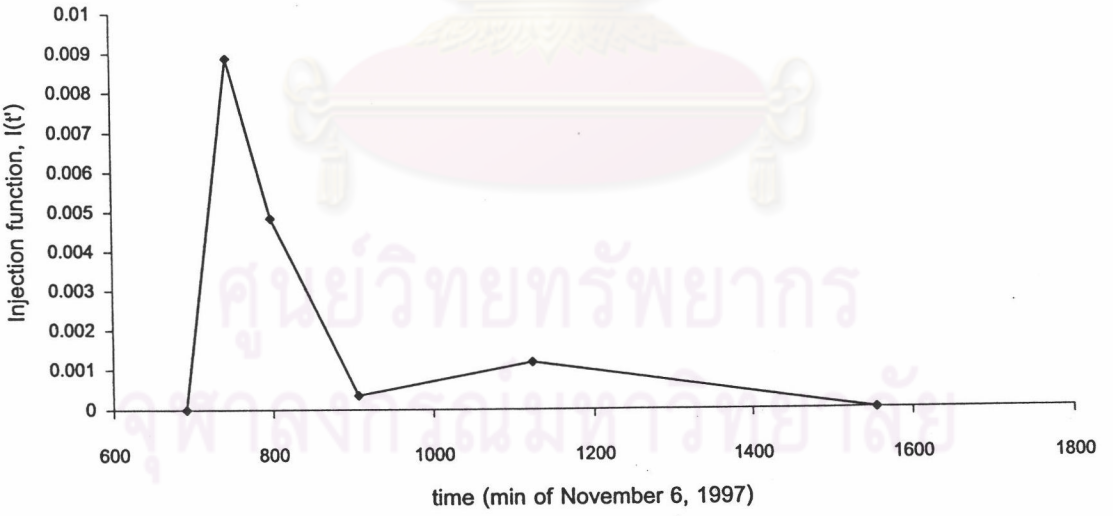

Figure 5.26: The injection function of iron at 23.6-36.3 MeV/n of the solar event on November 6, 1997 at the best-fit λ= 0.033 AU.

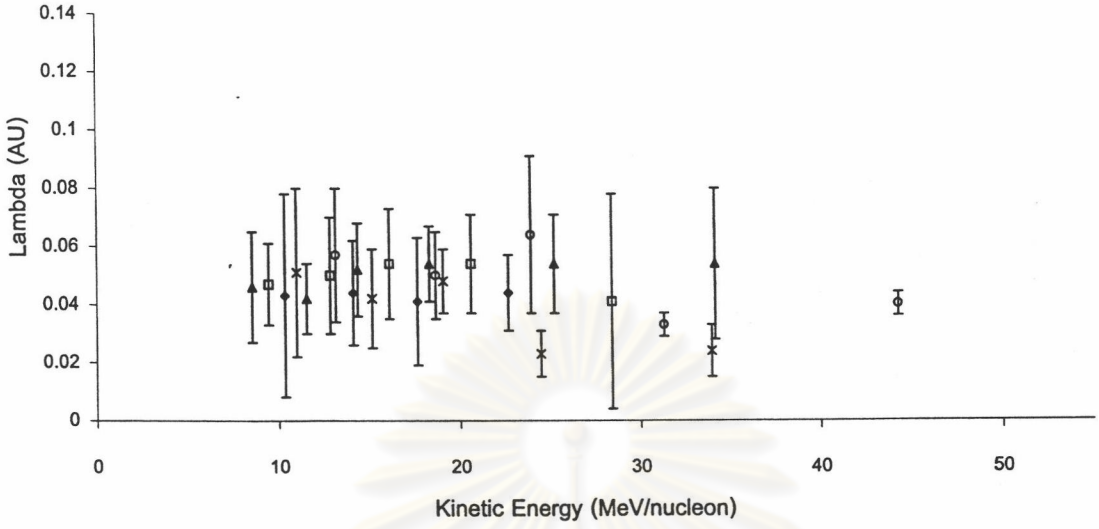

Figure 5.27: The summary results of the mean free path vs. energy per nucleon for each element for various energy values on November 6, 1997. Diamonds, circles, triangles, crosses, and squares indicate magnesium, iron, oxygen, silicon, and neon, respectively.

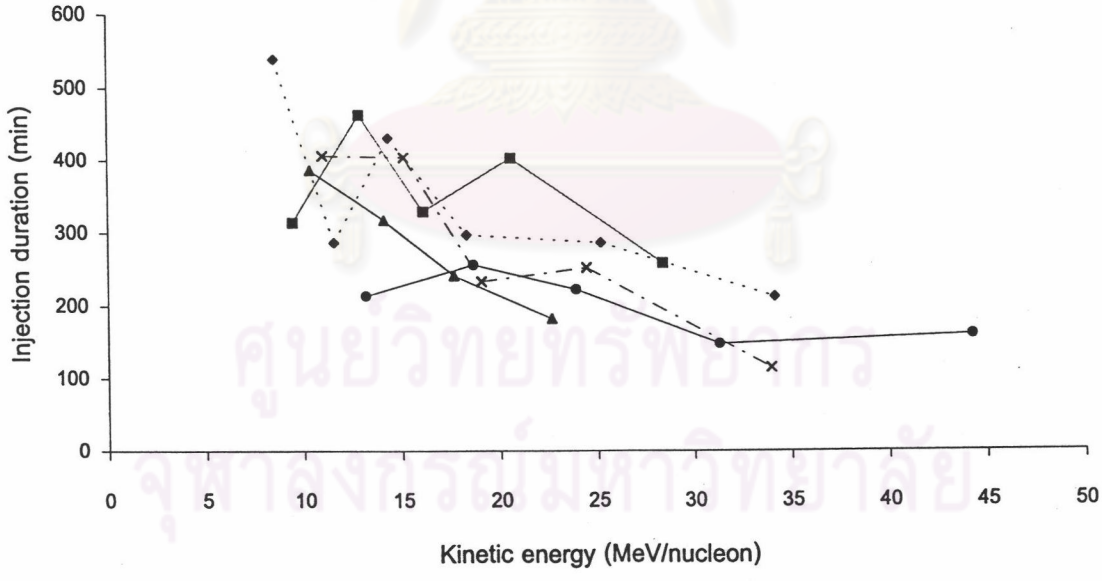

Figure 5.28: The injection function vs. kinetic energy of particles on November 6, 1997. Diamonds, squares, triangles, crosses, and circles indicate oxygen, neon, magnesium, silicon, and iron, respectively.

Element	Energy Band (MeV/n)	Mean Free Path (AU)	Injection Time (min)
Oxygen	7.1-10.0	0.046+/-0.019	539.564
	10.0-13.1	0.042+/-0.012	287.005
	13.1-15.6	0.052+/-0.016	431.8
	15.6-21.0	0.054+/-0.013	298.423
	21.0-29.4	0.054+/-0.017	287.386
	29.4-38.9	0.054+/-0.026	213.99
Neon	7.8-11.1	0.047+/-0.014	315.34
	11.1-14.6	0.05+/-0.02	464.239
	14.6-17.6	0.054+/-0.019	330.177
	17.6-23.6	0.054+/-0.017	404.128
	23.6-33.2	0.041+/-0.037	259.367
	33.2-44	0.0735+/-0.02	277.064
Magnesium	8.5-12.2	0.043+/-0.035	387.302
	12.2-16.0	0.044+-/0.018	318.22
	16.0-19.3	0.041+/-0.022	242.188
	19.3-26.0	0.044+/-0.013	183.29
Silicon	9.0-13.0	0.051+/-0.029	406.81
	13.0-17.3	0.042+/-0.017	404.56
	17.3-20.8	0.048+/-0.011	234.269
	20.8-28.1	0.023+/-0.008	253.05
	28.1-39.8	0.024+/-0.009	114.884
Iron	10.5-15.8	0.057+/-0.023	213.99
	15.8-21.5	0.05+/-0.015	257.35
	21.5-26.3	0.064+/-0.027	223.05
	26.3-36.3	0.033+/-0.004	147.97
	36.3-52.2	0.04+/-0.004	160.66

Table 5.1: Fitting results for November 6, 1997.

5.4 Comparison of Results for Three Solar Events

Solving the transport equation for solar energetic particle transport, as well as fitting data for the solar events of interest, we found the best-fit mean free path of particles and their injection function for various types of particles and energy bands. The results for three solar events can be compared as shown in Table 5.2.

In addition to the key results of each event, in comparison we found that:

1. We found that λ_r is roughly constant for a single event, as shown in Table 5.1 and Figure 5.27 for the Nov. 6, 1997 event, where λ_r is a important parameter of interplanetary transport. On the other hand, there are major variations from event to event. Physically, this implies that interplanetary scattering is approximately energy independent, but the level of scattering varies with time. This is consistent with results of Palmer (1982) and Bieber et al. (1994).

2. We found that the injection duration decreases with increasing energy as shown in Figure 5.28. This qualitative conclusion applies to the many fits performed for November 6, 1997, and also to the two other events as well. This implies that the injection duration of the solar energetic particles depends on the effects of acceleration at the CME while it is still in the corona or close to the Sun. In Figure 5.28, we found that while there are some fluctuations, overall the injection duration of the higher energy particles is shorter than for the lower energy particles. This means that the acceleration of these energetic particles by the CME-driven shock is greatest at the Sun, and particles are also accelerated while the CME propagates outward from the Sun, and the CME-driven shock lost the ability to accelerate the solar energetic particles after traveling a certain distance from the Sun (Kahler et al. 1990). Our results here are consistent with

those of Ruffolo, Khumlumlert, and Youngdee (1998), showing that high-energy particles are produced closer to the Sun, and the CME-driven shock loses the ability to accelerate particles to high energy more quickly than for lower energies.

3. Our types of automated and objective fitting rely on χ^2 minimization and not eyeball evaluation as in most previous works. We can use the techniques in this work for studying the solar energetic particle transport and fitting the spacecraft or ground-based data for various types of particles and energy bands as well.

Date of event	July 9, 1996	November 6, 1997	July 14, 2000
Particle	Proton	Fe, Ne, Si, O, Mg	Proton
Kinetic energy	123 keV	~7-100 MeV/nucleon	1 GeV
The X-ray duration (reference)	~ 5 min (decay time) Laitinen, T et al., Astronomy and Astrophysics, vol. 360, p. 729-741 (2000)	< 1 hour (10% of its peak intensity) Cliver et al., American Geophysical Union Fall Meeting 2001 #SH31C-09	< 25 min (decay time) Share, G. H. et al. American Geophysical Union, Spring Meeting 2001 #SH62B-09
CME ?	Yes	Yes	Yes
Special transport considerations	Use Compton-Getting transformation	No	Use the bottleneck configuration in Archimedean spiral magnetic field.
The mean free path from fitting	0.42 AU	~0.02-0.05 AU	0.18 AU
The injection time from fitting	274 min	114 - 540 min	7 min
Key result	We can fit data on low energy particles from the Sun.	We can systematically analyze data on many elements and energy bands, injection duration decreases with energy.	First detailed evidence of interplanetary mirroring of energetic particles.

Table 5.2: Comparison of results for three solar events.